HHS Public Access

Author manuscript

J Immunol. Author manuscript; available in PMC 2018 March 15.

Published in final edited form as:

J Immunol. 2017 March 15; 198(6): 2366–2373. doi:10.4049/jimmunol.1601471.

Loss of CMAH During Human Evolution Primed the Monocyte-Macrophage Lineage Towards a More Inflammatory and Phagocytic State

Jonathan J. Okerblom[*,†], **Flavio Schwarz**[*,†], **Josh Olson**[‡], **William Fletes**[*,§], **Syed Raza Ali**[*,‡], **Paul T. Martin**[¶], **Christopher K. Glass**[*,†], **Victor Nizet**[*,‡], and **Ajit Varki**[*,†]

[*]Glycobiology Research and Training Center, University of California, San Diego, CA, USA

[†]Departments of Medicine and Cellular and Molecular Medicine, University of California, San Diego, CA, USA

[‡]Department of Pediatrics and Skaggs School of Pharmacy and Pharmaceutical Sciences, University of California, San Diego, CA, USA

[§]Initiative for Maximizing Student Development (IMSD) Program, University of California, San Diego, CA, USA

[¶]Departments of Pediatrics, Physiology and Cell Biology, Ohio State University College of Medicine, Columbus, OH, USA and Center for Gene Therapy, The Research Institute at Nationwide Children's Hospital, Columbus, OH, USA

Abstract

Humans and chimpanzees are more sensitive to endotoxin than mice or monkeys, but any underlying differences in inflammatory physiology have not been fully described or understood. We studied innate immune responses in *Cmah*$^{-/-}$ mice, emulating human loss of the gene encoding production of Neu5Gc, a major cell surface sialic acid. *CMAH* loss occurred ~2-3 million years ago, after the common ancestor of humans and chimpanzees, perhaps contributing to speciation of the genus *Homo*. *Cmah*$^{-/-}$ mice manifested a decreased survival in endotoxemia following bacterial lipopolysaccharide (LPS) injection. Macrophages from *Cmah*$^{-/-}$ mice secreted more inflammatory cytokines with LPS-stimulation and showed more phagocytic activity. Macrophages and whole blood from *Cmah*$^{-/-}$ mice also killed bacteria more effectively. Metabolic re-introduction of Neu5Gc into *Cmah*$^{-/-}$ macrophages suppressed these differences. *Cmah*$^{-/-}$ mice also showed enhanced bacterial clearance during sub-lethal lung infection. Although monocytes and monocyte-derived macrophages from humans and chimpanzees exhibited marginal differences in LPS responses, human monocyte-derived macrophages killed *E. coli* and ingested *E. coli* bioparticles better. Metabolic re-introduction of Neu5Gc into human macrophages suppressed these differences. While multiple mechanisms are likely involved, one cause is altered expression of C/EBPβ, a transcription factor affecting macrophage function. Loss of Neu5Gc in *Homo* likely had complex effects on immunity, providing greater capabilities to clear sub-lethal bacterial challenges, possibly at the cost of endotoxic shock risk. This trade-off may have provided a

Address correspondence to a1varki@ucsd.edu, Mail: UC San Diego, La Jolla, CA 92093-0687, Phone: (858) 534-2214, Fax: (858) 534-5611.

selective advantage when *Homo* transitioned to butchery using stone tools. The findings may also explain why the *Cmah*$^{-/-}$ state alters severity in mouse models of human disease.

Introduction

Approximately two to three million years ago (mya), our ancestors inactivated the gene encoding CMP-Neu5Ac hydroxylase (CMAH), an enzyme that adds a single oxygen atom to the *N*-acetyl group of the sialic acid *N*-acetylneuraminic acid (Neu5Ac), converting it to the hydroxylated form, *N*-glycolylneuraminic acid (Neu5Gc) (1). Since *CMAH* is homozygously pseudogenized in all humans, this mutation resulted in the loss of tens of millions of hydroxyl groups from the plasma membrane surface of most cell types (2). The overall consequences of human *CMAH* loss are being investigated by multiple approaches, including studies of mice harboring a human-like mutation in *Cmah* (3). Studies in such mice indicate that partial reproductive incompatibility due to Neu5Gc loss ~2-3 mya likely contributed to speciation of the genus *Homo* (4), which also happens to be a time when the risk of injury and novel infections may have also increased due to scavenging and hunting, involving butchery of animal carcasses with stone tools (5–10). We also reported a difference in human and chimpanzee lymphocyte activation (11, 12) and showed that feeding Neu5Gc (which is metabolically incorporated and displayed) to activated human lymphocytes suppresses their proliferative response (13). In addition loss of *Cmah* function accelerates the pathological progression of the mdx and LGMD2D mouse models of human muscular dystrophy (14, 15), concomitant with increased CD68^{+} innate immune cell recruitment to muscles and increased muscle production of inflammatory cytokines, including IL-1β and MCP-1.

Tissue injury invokes a complex repair and regenerative response, which is substantially facilitated and potentiated by the resident and recruited host innate immune system (16–22). Classically, the first responders to tissue injury are the resident macrophage population, followed by neutrophils, which are rapidly recruited from circulating blood to the site of injury (23, 24). Blood monocytes are also recruited and produce many inflammatory components (25–27). The next wave of innate immune cell recruitment involves a more complex anti-inflammatory macrophage population (28–30), which facilitates wound healing (31–33). Dysregulation of these inflammatory and anti-inflammatory pathways during chronic disorders can lead to unrestrained inflammation, ultimately leading to an increase in tissue fibrosis and in some cases, tissue loss (34–37).

Toll-like receptors (TLRs), which are innate pattern recognition receptors, are master regulators of the innate inflammatory status of cells (38, 39). TLRs also recognize and potentiate the first line of host defense against pathogens. Recently, Toll-like receptor 4 (TLR4) has been implicated in the pathology of muscular dystrophy, wherein muscles are in a chronically inflamed state (18). Classically, lipopolysaccharide (LPS), which can be released from the outer membrane of gram-negative bacteria, stimulates the production and secretion of pro-inflammatory cytokines such as TNFα, IL-6, and IL-1β (40–44). LPS is recognized by TLR4, which is part of the LPS receptor complex, along with CD14 and

MD-2. TLR4 contains 9 N-linked glycans in its ectodomain, two of which are required for its membrane localization and others that are important for proper LPS binding (45).

Sialic acids such as Neu5Ac and Neu5Gc commonly terminate these N-linked glycan chains and their density and signaling influence can be affected by the action of endogenous neuraminidase 1 (a sialidase) (46–49). Sialic acid-bearing glycosphingolipids (gangliosides) that densely populate lipid rafts on cell membranes have also been shown to directly influence the translocation of TLR4 into lipid rafts after LPS stimulation (50). The specific impact of human CMAH/Neu5Gc loss has not been explored in these systems. Therefore, we focused our investigation on the impact of *Cmah* loss on innate immune responses, as a model for how Neu5Gc loss could have altered inflammatory physiology during the evolution of genus *Homo*.

Materials and Methods

Isolation of monocytes

Chimpanzee blood samples were collected into EDTA-containing tubes during routine non-invasive health screens of chimpanzee subjects at the Yerkes National Primate Center, Emory University, Atlanta, GA under local IRB approval by Emory University). All collections were made under the rules prevailing prior to the Sept 15, 2015 designation of captive chimpanzees as endangered species (51). Chimpanzee blood samples were shipped overnight on ice to the University of California, San Diego. Human blood was collected at about the same time into identical tubes from healthy volunteer donors (following informed consent, under the approval from the University of California, San Diego Human Subjects IRB), and stored overnight on ice, to ensure similar treatment conditions prior to analysis. All health and safety issues related to handling of human and non-human primate samples are covered by an Institutional biosafety approval from the University of California San Diego Environmental Health and Safety Committee. All individuals who handle the samples received the required training regarding precautions for blood-borne pathogens. PBMCs were separated over Ficoll-Paque PLUS (GE Healthcare, Uppsala, Sweden), followed by positive selection for monocytes using a CD14 MACS system (Miltenyi Biotech, Bergisch Gladbach, Germany), according to the manufacturer's protocol.

Intracellular TNF labeling & cytokine release detection

One million monocytes were seeded per well of a 48-well plate or 100,000 macrophages per well in a 24 well plate were stimulated with varying doses of LPS, while unstimulated cells served as negative controls. Stimulation for all assays was conducted at 37°C and 5% CO2, in the presence of 0.5 mg/ml brefeldin A (Sigma-Aldrich, St. Louis, MO) to inhibit cellular cytokine release. The intracellular cytokine content was determined after 4 hours of stimulation. Briefly, cells were fixed and permeabilized using Fix Buffer I and Perm/Wash Buffer I (BD Biosciences, San Jose, CA) and stained for intracellular TNFα. Samples were analyzed with a FACSCalibur (BD Biosciences). The frequencies of cytokine-positive cells were determined by subsequent analysis using FlowJo software (TreeStar).

Animals

All animal experiments were conducted under approved protocols and according to the regulations and guidelines of the Institutional Animal Care and Use Committee at the University of California, San Diego. Male and Female Cmah$^{-/-}$ C57/B6 (Harlan) mice 8-10 weeks were injected with 30 mg/kg LPS (Sigma, L2880, Lot# 044M4004V) and monitored over the period of 72 hours for mortality.

Lung Infection Model

The murine sub-lethal lung infection model was performed with slight modifications, as previously described (52). *E. coli* cultures were grown overnight in LB at 37 °C with shaking and then re-grown in the morning in fresh LB to a concentration of OD600 = 0.4. Bacteria were washed twice with PBS via centrifugation at 3220 ×g at room temperature and concentrated in PBS to yield 5×10^6 CFU in the 40 μL, the inoculation volume. Mice were anesthetized with 100 mg/kg ketamine and 10 mg/kg xylazine. Once sedated, the vocal chords were visualized using an operating otoscope (Welch Allyn) and 40μL of bacteria was instilled into the trachea during inspiration using a plastic gel loading pipette tip. Mice were placed on a warmed pad for recovery. Mice were sacrificed with CO_2 for bacterial counts 24 h after infection. To enumerate total surviving bacteria in the lungs, both lung lobes were removed and placed in a 2 mL sterile micro tube (Sarstedt) containing 1 mL of PBS and 1 mm silica beads (Biospec). Lungs were homogenized by shaking twice at 6000 rpm for 1 min using a MagNA Lyser (Roche), with the specimens placed on ice as soon as they were harvested. Aliquots from each tube were serially diluted for CFU enumeration on LB plates.

Mouse bone marrow derived macrophages

BMDMs were isolated from the femurs and tibia of 8-to-12-week-old WT and Cmah$^{-/-}$ C57BL/6 mice. Femurs and tibias were flushed with room-temperature Dulbecco's modified Eagle's medium (DMEM), and precursor cells were cultured in RPMI–20% fetal bovine serum (FBS), 1% penicillin-streptomycin, and 50 ng/mL M-CSF at 37°C in 5% CO_2 for 7 days, with changes of media on day 4. One day prior to LPS stimulation, cells were lifted with 5 mM EDTA and 300,000 cells/well were seeded in a 24-well plate in RPMI–10% FBS.

Mouse peritoneal macrophages

Peritoneal macrophages from 8-to-12-week-old WT and Cmah$^{-/-}$ C57BL/6 mice were harvested 4 days after 2.5 mL of 3% thioglycolate intraperitoneal injection. A total volume of 10 mL ice cold PBS was used to extract 7-8 mL of peritoneal lavage. Cells were separated by adherence overnight, washed with PBS, lifted with 5 mM EDTA, then 300,000 cells/well in a 24-well plate or 100,000 cells/well in a 96-well plate were seeded in RPMI–10% FBS.

Human and Chimpanzee monocyte-derived macrophages

Human or chimpanzee PBMCs isolated from 20 mL of blood were plated at one 24 well. Monocytes were separated by overnight adhesion in RPMI containing 10% FBS and 1% Pen/Strep and cell culture media was carefully replaced with RPMI containing 10%FBS and 100 ng/mL Human M-CSF without washing. Cells were allowed to differentiate in the

presence of M-CSF for 5 days. Additional RPMI + 10%FBS + 100 ng/mL Human M-CSF was added when needed in order to maintain normal pH. After 5 days, adherent cells were washed twice with PBS and resuspended in the appropriate experimental conditions.

Quantification of Sialic Acid Content by DMB-HPLC

Quantification of Sia content and type on acid-hydrolyzed samples of vertebrate tissues, polymers, and disaccharides was done using previously described methods of DMB derivatization at 50°C for 2.5 h (53), followed by HPLC-fluorometry on a Phenomenex C18 column using an isocratic elution in 85% water, 7% methanol, and 8% acetonitrile.

Macrophage Phagocytosis Assay

pHrodo Red *E. coli* (ThermoFisher, P35361) and *S. aureus* (ThermoFisher, A10010) Bioparticles Conjugates for Phagocytosis were used exactly as indicated by manufacturer's protocol. 100,000 peritoneal macrophages/well were incubated with 100 uL pHrodo Bioparticle suspension for 1 or 2 hours. For confocal microscopy, cells were fixed in 2% PFA/PBS at 4°C, then imaged by fluorescent microscopy at the exact same exposure.

Macrophage Bacterial Killing Assay

A single *E. coli K12* colony was inoculated in LB and incubated overnight on a shaker at 37°C. The next day, inoculum was diluted 1:100 and optical density (OD) was monitored up to 0.4 (corresponding to ~2×10^8 CFU/mL). Bacteria was washed once with PBS and resuspended in appropriate cell culture media. Bacteria was then added to plates, centrifuged at 500g for 10 min, and then incubated with cells at 37°C. Macrophages were then lysed with 0.05% TX-100, scraped with a rubber stopper, and plated. Neutrophils and whole blood were diluted in the same lysis buffer before plating. Inoculum and all other samples were plated at four different dilutions (10^{-1} – 10^{-4}) in triplicates. Percent survival was calculated as the experimental sample CFU divided by the initial inoculum CFU.

LPS Binding Assay

Peritoneal lavage from WT and $Cmah^{-/-}$ mice was resuspended at 2 million cells/mL in cold PBS and handled on ice. Cell fluorescence was collected in real time by flow cytometry at a rate of approximately 1,000/second for 10 seconds. Tube was then removed, 10 ug fluorescent LPS (Sigma, F8666) was added followed by a quick vortex. Tube was then immediately returned to the flow cytometer and measured in real time for an additional 2 minutes.

RNA-Seq

Total RNA was assessed for quality using an Agilent Tapestation, with RNA Integrity Numbers (RIN) ranging from 8.8 to 10.0. RNA libraries were generated using Illumina's TruSeq Stranded mRNA Sample Prep Kit using 100 ng of RNA following manufacturer's instructions, modifying the shear time to 5 minutes. RNA libraries were multiplexed and sequenced with 50 basepair (bp) single end reads (SR50) to a depth of approximately 20 million reads per sample on an Illumina HiSeq4000.

Statistical analysis

Error data represents standard errors of the means (SEM) of the results. When comparing WT vs. Cmah$^{-/-}$ or human vs. chimpanzee macrophages, statistical analysis was performed using two-way analysis of variance (ANOVA) followed by the Tukey's multiple comparisons test. For Neu5Ac and Neu5Gc feeding experiments on the same cells, Student's paired two-tailed *t*-test was performed. For the survival assay, statistical significance was evaluated using the Logrank (Mantel-Cox) test with a 95% confidence interval. (Graph Pad Prism, version 7.0a). * ($P < 0.05$), ** ($P < 0.01$), and *** ($P < 0.001$) represent statistical significance. For RNA-seq, q values were determined using DESeq2 differential expression analysis.

Results

Mice and Macrophages with a Human-like loss of Neu5Gc Show Enhanced Sensitivity to LPS Activation

To simulate the immediate effects CMAH loss in the human lineage ~2-3 mya, we compared WT and congenic *Cmah*$^{-/-}$ mice (Figure 1A). First, we determined the impact of Neu5Gc on the LPS response *in vivo* by injecting WT and *Cmah*$^{-/-}$ mice with potentially lethal doses of LPS and monitoring survival. At multiple doses, *Cmah*$^{-/-}$ mice exhibited a significant reduction in survival rate compared to WT controls (Figure 1B-D). Next we assessed the specific role of Neu5Gc in the macrophage inflammatory response by comparing LPS responses of macrophages derived from bone marrow or the peritoneal cavity. After 24 hours of stimulation, bone marrow-derived macrophages from *Cmah*$^{-/-}$ mice produced more inflammatory IL-6 (Figure 1E) and peritoneal macrophages secreted higher levels of MCP-1 (Figure 1F). Notably, these phenotypes were not due to differential expression of the LPS receptor TLR4 (Supp. Fig. 1A) or changes in LPS binding (Supp. Fig 1B). We concluded that macrophages from *Cmah*$^{-/-}$ Mice exhibit higher sensitivity to LPS, possibly due to differences in signaling.

Macrophages from Mice with a Human-like loss of Neu5Gc Show Increased Phagocytosis and Killing of Bacteria

We next explored a more functionally relevant benefit of a stronger innate inflammatory response: the ability to clear and kill bacteria. We checked the capability of mouse peritoneal macrophages to kill *E. coli* and observed a ~50% reduction in recovery of bacteria incubated with *Cmah*$^{-/-}$ macrophages (Figure 2A). A similar increase in bacterial killing was observed in heparinized whole blood from *Cmah*$^{-/-}$ mice compared to WT controls. (Figure 2B). To prove that the observed differences were related to the absence of Neu5Gc, we studied peritoneal macrophages isolated from *Cmah*$^{-/-}$ mice that had been fed equal concentrations of either Neu5Ac or Neu5Gc. This approach allows experimental manipulation of cells from the same individual to generate expression of either cell surface Neu5Ac or Neu5Gc, for direct comparison to each other. Free sialic acids in the media can only be taken up through macropinocytosis and utilized by the cell if they are transported into the cytosol by the endolysosomal transporter sialin (54). Once there, free Neu5Ac or Neu5Gc must be transported to the nucleus to be CMP-activated (55) and then to the Golgi lumen to be conjugated onto glycoproteins or glycolipids. The half-life of free sialic acids fed to cells is

~4 days (56), so most of it should be utilized in this way after feeding. However, sialic acid degradation to their acetate (from Neu5Ac) and glycolate (from Neu5Gc) metabolites does occur during the constant recycling of endogenous Neu5Ac or Neu5Gc sialic acids during maintenance of steady state (56–59). Similar to results observed between WT and Cmah$^{-/-}$ mice, the feeding of Neu5Gc to peritoneal macrophages isolated from *Cmah*$^{-/-}$ mice indeed increased their Neu5Gc content (Supp. Fig 3A) and suppressed their capability to kill bacteria (Figure 2C).

To determine the effect of Cmah loss on bacterial killing *in vivo*, we infected the lungs of WT and *Cmah*$^{-/-}$ mice with *E. coli* K12 bacteria via intranasal inoculation. At 24h, *Cmah*$^{-/-}$ mice exhibited a greater capability to clear *E. coli* K12 from the lungs *in vivo* compared to WT controls (Figure 2D). WT and *Cmah*$^{-/-}$ peritoneal macrophages were also incubated with *S. aureus* bioparticles that fluoresce when internalized into phagosomes and we observed a ten-fold increase in macrophage phagocytosis of the fluorescent bacterial particles in *Cmah*$^{-/-}$ macrophages (Figure 2E-F). Taken together, this data suggests that loss of Neu5Gc leads to increased phagocytic activity and bacterial clearance during infection.

Human Innate Immune Cells Show increased Phagocytosis and Killing of Bacteria Relative to Chimpanzees, which is Suppressed by Neu5Gc feeding

Chimpanzees have intact CMAH function and express high levels of Neu5Gc on their cell surfaces (60). However, they have diverged independently for ~6-7 mya since the common ancestor with humans, and also have a significantly higher genetic diversity. The availability of samples was limited to chimpanzees in captivity undergoing routine blood testing during annual health checks (prior to the Sept 15, 2015 restriction on such ethically reasonable studies) (51). We noted an unexplained technical pitfall associated with positively enriching for chimpanzee CD14^{+} PBMCs, since (unlike human samples) they are commonly contaminated with ~70% neutrophils. Therefore, we compared innate inflammatory response of limited samples of chimpanzee monocytes to those of humans and conducted the rest of our limited comparisons with monocyte-derived macrophages. Monocyte-derived macrophages from humans incubated with *E. coli* exhibited a greater killing capacity compared to chimpanzee controls (Figure 3A). A similar difference in bacterial killing was observed in whole blood from chimpanzees and humans inoculated with *E. coli* (K12) bacteria (Figure 3B). Similar to *Cmah*$^{-/-}$ mouse macrophages, feeding human monocytes with Neu5Gc substantially reduced their capacity of killing bacteria (Figure 3C). We tested the same human and chimpanzee monocyte-derived macrophages for both the intracellular TNFα expression after LPS stimulation and the phagocytosis of *E. coli* or *S. aureus* bioparticles. Macrophages were incubated with LPS in the presence of brefeldin A for 4h or with the bioparticles for 1h in the presence of autologous heat denatured serum. Although we did not observe a statistically significant difference in intracellular TNFα (Figure 3D), the same human cells exhibited substantially greater phagocytosis of both *E. coli* and *S. aureus* bioparticles compared to chimpanzee cells (Figure 3E-F).

Peripheral blood monocytes were stimulated with LPS for 4h and intracellular TNFα production was measured by flow cytometry. The percentage of TNFα positive cells were also measured by quantifying intracellular TNFα levels above baseline levels. Human

$CD14^+$ monocytes showed a marginal increase in TNFα production compared to chimpanzees *ex vivo,* but this difference was not statistically significant (Supp Fig 2A-B). Considerable variation was also seen, as expected for the individuals from outbred species with varying genetic backgrounds, and environmental conditions.

We next differentiated human monocytes into macrophages while feeding the same cells either Neu5Ac or Neu5Gc for 4 days. We observed a significant effect on intracellular TNFα expression (Figure 4A-B) and *E. coli* bioparticle phagocytosis (Figure 4C-D) in Neu5Gc fed macrophages compared to Neu5Ac fed macrophages.

Neu5Gc Containing Mouse Macrophages Show Differential Expression of C/EBPβ

To determine if Neu5Ac or Neu5Gc feeding differentially altered gene expression, we performed RNAseq on macrophages from $Cmah^{-/-}$ mice that had been fed either Neu5Ac or Neu5Gc for 3 days (Fig. 5A). Although several of the 36 genes that showed significant differential expression (Supp. Table 1) could be affecting macrophage function, C/EBPβ (Fig. 5B) was of major interest because of its role in macrophage development and bacterial killing (61, 62). Therefore, we examined the protein expression of LAP (a 34 kDa C/EBPβ isoform that is transcriptionally active in macrophages) and found that LAP expression is elevated in $Cmah^{-/-}$ peritoneal macrophages compared to WT controls (Fig. 5C-D).

Discussion

We have suggested that initial hominin loss of CMAH may have been selected by an infectious agent, such as the malarial sporozoite recognition of erythrocyte sialic acids (60), and was then fixed relatively rapidly in a new population by virtue of cryptic female choice, mediated by intrauterine anti-Neu5Gc antibodies, selecting against ancestral Neu5Gc-positive sperm and/or embryos (4). Here we present data suggesting that fixation of the *CMAH*-null state may have then been beneficial for the transition of these hominins towards increased tool usage, butchery of carcasses, and exposure to novel pathogens. Approximately 2-3 mya, when *CMAH* loss is likely to have been fixed in our lineage (1), the fossils of late *Australopithecus* and early *Homo* are found surrounded by Oldowan stone tools, presumably used to break bones and eat nutrient rich bone marrow (5, 6, 8, 63). This activity likely resulted in superficial injuries, combined with exposure to new bacterial pathogens, potentially leading to a greater prevalence of infection.

Under these novel circumstances, the ability to kill and clear sublethal doses of bacteria at a greater capacity could have been beneficial for the utilization of stone tools and the consumption of other animals. On the other hand, just as other ancestral mutations have become deleterious for specific modern pathologies (64, 65), CMAH loss may be a deleterious contributor to endotoxemia in humans today who experience overwhelming infections and sepsis (66).

Understanding the immediate effect of CMAH loss on ancient hominin physiology is impossible. Our best efforts are to compare humans vs. chimpanzees *ex vivo* and $Cmah^{-/-}$ vs. WT mice *ex vivo* and *in vivo*. When comparing humans and chimpanzee macrophages *ex vivo* we see a non-significant difference in inflammatory responses in the same conditions

where we see significant differences in bacterial killing and phagocytosis. When studying the immediate effects of Cmah loss in mice, we see similar results: profound effects on bacterial killing, yet a relatively mild inflammatory phenotype *ex vivo.* Importantly, our experimental evidence also illustrates an increased sensitivity of *Cmah*$^{-/-}$ mice to endotoxic shock *in vivo*, which could be due to multiple mechanisms and other cell types. More work is needed to determine if an altered innate immune response in *Cmah*$^{-/-}$ mice contributes to other observed phenotypes, such as delayed wound healing (3), greater inflammation and fibrosis in the mdx model of muscular dystrophy (14), and increased growth of transplanted human tumor cells (67). We speculate that these and other human chronic inflammatory states could be modeled in *Cmah*$^{-/-}$ mice.

Fully explaining all mechanisms underlying these phenotypic differences is complex and difficult. Given the global impact of eliminating tens of millions of N-glycolyl groups from cells via CMAH loss, there are multiple possible (and mutually non-exclusive) mechanisms contributing to our findings. For example, cytosolic degradation of excess Neu5Gc can result in generation of glycolate (instead of acetate generated from Neu5Ac breakdown) (56), with the possibility of a systematic alteration in cell metabolism. Previously published microarray data in WT and Cmah−/− mouse muscle implicated CREB1, C/EBPα, and C/EBPβ as candidate transcription factors affected by Cmah loss (14). Alterations in these transcription factors have been shown to affect both macrophage activation and systemic metabolism (61, 68–70) and appear to be differentially expressed and regulated in different tissue types of WT vs. Cmah−/− mice. C/EBPβ expression is also suppressed in macrophages fed Neu5Gc and C/EBPβ (NF-IL6) knockout mice are known to experience a drastic reduction in the capability of their monocytes to kill bacteria (62, 70, 71).

It is also possible that Neu5Gc loss altered cell surface neuraminidase activity. Multiple reports have implicated neuraminidase 1 (Neu1) as an important regulator of the TLR4 response (47) and we previously reported that neuraminidase 1 (Neu1) prefers Neu5Ac to Neu5Gc in the α2-8 linkages common in polysialic acids (72). The endogenous neuraminidase preference for α2-3 or α2-6 linked Neu5Ac and Neu5Gc, which are common on the surface of innate immune cells, needs further study. A further non-mutually exclusive possibility is that the loss of millions of hydrophilic cell surface hydroxyl groups on Neu5Gc (replaced by hydrophobic acetyl groups on Neu5Ac) led to global changes in cell surface biophysics, which could have global ramifications on cell surface receptor localization, clustering, and signaling. It is reasonable to hypothesize that the cell membranes of humans and Cmah$^{-/-}$ mice are overall more hydrophobic than chimpanzee or WT counterparts.. Further investigations are needed to determine if global changes in cell surface biophysics occur after Cmah loss.

Due to a limitation in the amount of samples combined with a high genetic variation, it is also difficult to study the differences in inflammatory physiology between humans and chimpanzees. Our results are consistent with previous studies that have established that humans and chimpanzees respond at the same order of magnitude to endotoxin (43, 73–76). However, direct comparisons of humans and chimpanzees with the same batch of LPS at multiple doses *in vivo* is no longer possible, nor is it possible to compare survival after endotoxic shock between humans and chimpanzees with the same batch and dose of

endotoxin. Limited evidence using different batches of *E. Coli* endotoxin could suggest a difference between humans and chimpanzees, but are not directly comparable. For example, peak serum TNFα (68 to 1,374 pg/mL) and IL-6 (72 to 2,820 pg/mL) secretion of humans in response to 2ng/kg *E. coli* endotoxin bolus injection (74) is more sensitive than the serum TNFα (188 ± 54 pg/mL) and IL-6 (138 ± 37 pg/mL) concentrations of chimpanzees in response to 4 ng/kg *E. coli* endotoxin bolus injection (73). Regardless, when we compared human and chimpanzee macrophages *ex vivo*, we did not observe a statistically significant difference in the inflammatory response to LPS in exactly the same conditions where we did observe a difference in both bacterial killing and bioparticle phagocytosis.

Furthermore, millions of years have passed since humans and chimpanzees diverged from each other (77, 78). Therefore, studying differences in *Cmah*$^{-/-}$ and WT mice allows for greater sample sizes with much less genetic variation. Overall, we observed similar results in Cmah$^{-/-}$ vs. WT mice as we did in humans vs. chimpanzees and *Cmah*$^{-/-}$ mice are useful as a model for human evolution as well as human disease susceptibility.

While much further work is needed to define the multiple consequences of CMAH/Neu5Gc loss during human evolution, our current work suggests that there were likely complex effects on innate immunity, apparently providing a greater capability to clear sub-lethal bacterial challenges, possibly at the cost of increased risk of endotoxic shock. These findings may also help explain why the *Cmah* null state alters disease severity in mouse models of human disease associated with inflammation, like muscular dystrophy. They are also relevant to future modeling of human infectious disease states in mice.

Supplementary Material

Refer to Web version on PubMed Central for supplementary material.

Acknowledgements

We thank Yuko Naito-Matsui, Anel Lizcano, and Shoib Siddiqui for help in the lab. RNA-seq was conducted at the IGM Genomics Center, University of California, San Diego, La Jolla, CA.

Footnote:

This work was supported by NIH grants R01GM32373 to A.V., R01AR060949 to P.M., and by the Mathers Foundation of New York. Blood samples from chimpanzees were provided by the Yerkes Primate Center, Atlanta, GA under NIH Base Grant ORIP/OD P51OD011132.

Abbreviations

CMAH	CMP-Neu5Ac hydroxylase
Neu5Gc	*N*-glycolylneuraminic acid
Neu5Ac	*N*-acetylneuraminic acid

References

1. Chou HH, Takematsu H, Diaz S, Iber J, Nickerson E, Wright KL, Muchmore EA, Nelson DL, Warren ST, Varki A. A mutation in human CMP-sialic acid hydroxylase occurred after the Homo-Pan divergence. Proc Natl Acad Sci USA. 1998; 95:11751–11756. [PubMed: 9751737]
2. Varki A, Gagneux P. Multifarious roles of sialic acids in immunity. Ann N Y Acad Sci. 2012; 1253:16–36. [PubMed: 22524423]
3. Hedlund M, Tangvoranuntakul P, Takematsu H, Long JM, Housley GD, Kozutsumi Y, Suzuki A, Wynshaw-Boris A, Ryan AF, Gallo RL, Varki N, Varki A. N-glycolylneuraminic acid deficiency in mice: implications for human biology and evolution. Mol Cell Biol. 2007; 27:4340–4346. [PubMed: 17420276]
4. Ghaderi D, Springer SA, Ma F, Cohen M, Secrest P, Taylor RE, Varki A, Gagneux P. Sexual selection by female immunity against paternal antigens can fix loss of function alleles. Proc Natl Acad Sci U S A. 2011; 108:17743–17748. [PubMed: 21987817]
5. Semaw S, Renne P, Harris JW, Feibel CS, Bernor RL, Fesseha N, Mowbray K. 2.5-million-year-old stone tools from Gona, Ethiopia. Nature. 1997; 385:333–336. [PubMed: 9002516]
6. Baird A, Costantini T, Coimbra R, Eliceiri BP. Injury, inflammation and the emergence of human-specific genes. Wound Repair Regen. 2016; 24:602–606. [PubMed: 26874655]
7. McPherron SP, Alemseged Z, Marean CW, Wynn JG, Reed D, Geraads D, Bobe R, Béarat HA. Evidence for stone-tool-assisted consumption of animal tissues before 3.39 million years ago at Dikika, Ethiopia. Nature. 2010; 466:857–860. [PubMed: 20703305]
8. Harmand S, Lewis JE, Feibel CS, Lepre CJ, Prat S, Lenoble A, Boës X, Quinn RL, Brenet M, Arroyo A, Taylor N, Clément S, Daver G, Brugal JP, Leakey L, Mortlock RA, Wright JD, Lokorodi S, Kirwa C, Kent DV, Roche H. 3.3-million-year-old stone tools from Lomekwi 3, West Turkana, Kenya. Nature. 2015; 521:310–315. [PubMed: 25993961]
9. Sayers K, Lovejoy CO. Blood, bulbs, and bunodonts: on evolutionary ecology and the diets of Ardipithecus, Australopithecus, and early Homo. Q Rev Biol. 2014; 89:319–357. [PubMed: 25510078]
10. O'Connell JF, Hawkes K, Lupo KD, Blurton Jones NG. Male strategies and Plio-Pleistocene archaeology. J Hum Evol. 2002; 43:831–872. [PubMed: 12473486]
11. Soto PC, Stein LL, Hurtado-Ziola N, Hedrick SM, Varki A. Relative over-reactivity of human versus chimpanzee lymphocytes: implications for the human diseases associated with immune activation. J Immunol. 2010; 184:4185–4195. [PubMed: 20231688]
12. Soto PC, Karris MY, Spina CA, Richman DD, Varki A. Cell-intrinsic mechanism involving Siglec-5 associated with divergent outcomes of HIV-1 infection in human and chimpanzee CD4 T cells. J Mol Med (Berl). 2012; 91:261–270. [PubMed: 22945238]
13. Buchlis G, Odorizzi P, Soto PC, Pearce OM, Hui DJ, Jordan MS, Varki A, Wherry EJ, High KA. Enhanced T cell function in a mouse model of human glycosylation. J Immunol. 2013; 191:228–237. [PubMed: 23709682]
14. Chandrasekharan K, Yoon JH, Xu Y, deVries S, Camboni M, Janssen PM, Varki A, Martin PT. A human-specific deletion in mouse Cmah increases disease severity in the mdx model of Duchenne muscular dystrophy. Sci Transl Med. 2010; 2:42ra54.
15. Martin PT, Camboni M, Xu R, Golden B, Chandrasekharan K, Wang CM, Varki A, Janssen PM. N-glycolylneuraminic acid deficiency worsens cardiac and skeletal muscle pathophysiology in alpha sarcoglycan-deficient mice. Glycobiology. 2013; 28:833–843.
16. Gurtner GC, Werner S, Barrandon Y, Longaker MT. Wound repair and regeneration. Nature. 2008; 453:314–321. [PubMed: 18480812]
17. Koh TJ, DiPietro LA. Inflammation and wound healing: the role of the macrophage. Expert Rev Mol Med. 2011; 13:e23. [PubMed: 21740602]
18. Giordano C, Mojumdar K, Liang F, Lemaire C, Li T, Richardson J, Divangahi M, Qureshi S, Petrof BJ. Toll-like receptor 4 ablation in mdx mice reveals innate immunity as a therapeutic target in Duchenne muscular dystrophy. Hum Mol Genet. 2015; 24:2147–2162. [PubMed: 25552658]

19. Brinkworth JF, Barreiro LB. The contribution of natural selection to present-day susceptibility to chronic inflammatory and autoimmune disease. Curr Opin Immunol. 2014; 31:66–78. [PubMed: 25458997]
20. De Maio A, Torres MB, Reeves RH. Genetic determinants influencing the response to injury, inflammation, and sepsis. Shock. 2005; 23:11–17. [PubMed: 15614125]
21. Medzhitov R. Origin and physiological roles of inflammation. Nature. 2008; 454:428–435. [PubMed: 18650913]
22. Tabas I, Glass CK. Anti-inflammatory therapy in chronic disease: challenges and opportunities. Science. 2013; 339:166–172. [PubMed: 23307734]
23. Klebanoff SJ, Kettle AJ, Rosen H, Winterbourn CC, Nauseef WM. Myeloperoxidase: a front-line defender against phagocytosed microorganisms. J Leukoc Biol. 2013; 93:185–198. [PubMed: 23066164]
24. Kim ND, Luster AD. The role of tissue resident cells in neutrophil recruitment. Trends Immunol. 2015; 36:547–555. [PubMed: 26297103]
25. Németh T, Mócsai A. Feedback Amplification of Neutrophil Function. Trends Immunol. 2016
26. Mogensen TH. Pathogen recognition and inflammatory signaling in innate immune defenses. Clin Microbiol Rev. 2009; 22:240–73. Table of Contents. [PubMed: 19366914]
27. Aderem A. Phagocytosis and the inflammatory response. J Infect Dis. 2003; 187(Suppl 2):S340–5. [PubMed: 12792849]
28. Soehnlein O, Lindbom L. Phagocyte partnership during the onset and resolution of inflammation. Nat Rev Immunol. 2010; 10:427–439. [PubMed: 20498669]
29. Varin A, Mukhopadhyay S, Herbein G, Gordon S. Alternative activation of macrophages by IL-4 impairs phagocytosis of pathogens but potentiates microbial-induced signalling and cytokine secretion. Blood. 2010; 115:353–362. [PubMed: 19880493]
30. Okabe Y, Medzhitov R. Tissue biology perspective on macrophages. Nat Immunol. 2016; 17:9–17. [PubMed: 26681457]
31. Deng B, Wehling-Henricks M, Villalta SA, Wang Y, Tidball JG. IL-10 triggers changes in macrophage phenotype that promote muscle growth and regeneration. J Immunol. 2012; 189:3669–3680. [PubMed: 22933625]
32. Kharraz Y, Guerra J, Mann CJ, Serrano AL, Muñoz-Cánoves P. Macrophage plasticity and the role of inflammation in skeletal muscle repair. Mediators Inflamm. 2013; 2013:491497. [PubMed: 23509419]
33. Burzyn D, Kuswanto W, Kolodin D, Shadrach JL, Cerletti M, Jang Y, Sefik E, Tan TG, Wagers AJ, Benoist C, Mathis D. A special population of regulatory T cells potentiates muscle repair. Cell. 2013; 155:1282–1295. [PubMed: 24315098]
34. Mann CJ, Perdiguero E, Kharraz Y, Aguilar S, Pessina P, Serrano AL, Muñoz-Cánoves P. Aberrant repair and fibrosis development in skeletal muscle. Skelet Muscle. 2011; 1:21. [PubMed: 21798099]
35. Lieber RL, Ward SR. Cellular mechanisms of tissue fibrosis. 4. Structural and functional consequences of skeletal muscle fibrosis. Am J Physiol Cell Physiol. 2013; 305:C241–52. [PubMed: 23761627]
36. Chovatiya R, Medzhitov R. Stress, inflammation, and defense of homeostasis. Mol Cell. 2014; 54:281–288. [PubMed: 24766892]
37. Nathan C, Ding A. Nonresolving inflammation. Cell. 2010; 140:871–882. [PubMed: 20303877]
38. Kanzler H, Barrat FJ, Hessel EM, Coffman RL. Therapeutic targeting of innate immunity with Toll-like receptor agonists and antagonists. Nat Med. 2007; 13:552–559. [PubMed: 17479101]
39. Moresco EM, LaVine D, Beutler B. Toll-like receptors. Curr Biol. 2011; 21:R488–93. [PubMed: 21741580]
40. Lu YC, Yeh WC, Ohashi PS. LPS/TLR4 signal transduction pathway. Cytokine. 2008; 42:145–151. [PubMed: 18304834]
41. Covert MW, Leung TH, Gaston JE, Baltimore D. Achieving stability of lipopolysaccharide-induced NF-kappaB activation. Science. 2005; 309:1854–1857. [PubMed: 16166516]

42. Lawrence T, Bebien M, Liu GY, Nizet V, Karin M. IKKalpha limits macrophage NF-kappaB activation and contributes to the resolution of inflammation. Nature. 2005; 434:1138–1143. [PubMed: 15858576]
43. Brinkworth JF, Pechenkina EA, Silver J, Goyert SM. Innate immune responses to TLR2 and TLR4 agonists differ between baboons, chimpanzees and humans. J Med Primatol. 2012
44. Warren HS, Fitting C, Hoff E, Adib-Conquy M, Beasley-Topliffe L, Tesini B, Liang X, Valentine C, Hellman J, Hayden D, Cavaillon JM. Resilience to bacterial infection: difference between species could be due to proteins in serum. J Infect Dis. 2010; 201:223–232. [PubMed: 20001600]
45. Da Silva Correia J, Ulevitch RJ. MD-2 and TLR4 N-linked glycosylations are important for a functional lipopolysaccharide receptor. J Biol Chem. 2002; 277:1845–1854. [PubMed: 11706042]
46. Pshezhetsky AV, Ashmarina LI. Desialylation of surface receptors as a new dimension in cell signaling. Biochemistry (Mosc). 2013; 78:736–745. [PubMed: 24010837]
47. Pshezhetsky AV, Hinek A. Where catabolism meets signalling: neuraminidase 1 as a modulator of cell receptors. Glycoconj J. 2011; 28:441–452. [PubMed: 21928149]
48. Abdulkhalek S, Amith SR, Franchuk SL, Jayanth P, Guo M, Finlay T, Gilmour A, Guzzo C, Gee K, Beyaert R, Szewczuk MR. Neu1 sialidase and matrix metalloproteinase-9 cross-talk is essential for Toll-like receptor activation and cellular signaling. J Biol Chem. 2011; 286:36532–36549. [PubMed: 21873432]
49. Chen GY, Brown NK, Wu W, Khedri Z, Yu H, Chen X, van de Vlekkert D, D'Azzo A, Zheng P, Liu Y. Broad and direct interaction between TLR and Siglec families of pattern recognition receptors and its regulation by Neu1. Elife. 2014; 3:e04066. [PubMed: 25187624]
50. Nikolaeva S, Bayunova L, Sokolova T, Vlasova Y, Bachteeva V, Avrova N, Parnova R. GM1 and GD1a gangliosides modulate toxic and inflammatory effects of E. coli lipopolysaccharide by preventing TLR4 translocation into lipid rafts. Biochim Biophys Acta. 2015; 1851:239–247. [PubMed: 25499607]
51. Grimm D. Animal Welfare. New rules may end U.S. chimpanzee research. Science. 2015; 349:777. [PubMed: 26293932]
52. Revelli DA, Boylan JA, Gherardini FC. A non-invasive intratracheal inoculation method for the study of pulmonary melioidosis. Front Cell Infect Microbiol. 2012; 2:164. [PubMed: 23267442]
53. Manzi AE, Diaz S, Varki A. High-pressure liquid chromatography of sialic acids on a pellicular resin anion-exchange column with pulsed amperometric detection: A comparison with six other systems. Anal Biochem. 1990; 188:20–32. [PubMed: 2221361]
54. Bardor M, Nguyen DH, Diaz S, Varki A. Mechanism of uptake and incorporation of the non-human sialic acid N-glycolylneuraminic acid into human cells. J Biol Chem. 2005; 280:4228–4237. [PubMed: 15557321]
55. Kean EL, Munster-Kuhnel AK, Gerardy-Schahn R. CMP-sialic acid synthetase of the nucleus. Biochim Biophys Acta. 2004; 1673:56–65. [PubMed: 15238249]
56. Bergfeld AK, Pearce OM, Diaz SL, Pham T, Varki A. Metabolism of Vertebrate Amino Sugars with N-Glycolyl Groups: elucidating the intracellular fate of the non-human sialic acid N-glycolylneuraminic acid. J Biol Chem. 2012; 287:28865–28881. [PubMed: 22692205]
57. Margolis RK, Margolis RU. The turnover of hexosamine and sialic acid in glycoproteins and mucopolysaccharides of brain. Biochim Biophys Acta. 1973; 304:413–420. [PubMed: 4268021]
58. Ledeen RW, Skrivanek JA, Tirri LJ, Margolis RK, Margolis RU. Gangliosides of the neuron: localization and origin. Adv Exp Med Biol. 1976; 71:83–103. [PubMed: 59538]
59. Ferwerda W, Blok CM, Heijlman J. Turnover of free sialic acid, CMP-sialic acid, and bound sialic acid in rat brain. J Neurochem. 1981; 36:1492–1499. [PubMed: 7264646]
60. Martin MJ, Rayner JC, Gagneux P, Barnwell JW, Varki A. Evolution of human-chimpanzee differences in malaria susceptibility: relationship to human genetic loss of N-glycolylneuraminic acid. Proc Natl Acad Sci U S A. 2005; 102:12819–12824. [PubMed: 16126901]
61. Huber R, Pietsch D, Panterodt T, Brand K. Regulation of C/EBPβ and resulting functions in cells of the monocytic lineage. Cell Signal. 2012; 24:1287–1296. [PubMed: 22374303]
62. Tanaka T, Akira S, Yoshida K, Umemoto M, Yoneda Y, Shirafuji N, Fujiwara H, Suematsu S, Yoshida N, Kishimoto T. Targeted disruption of the NF-IL6 gene discloses its essential role in

bacteria killing and tumor cytotoxicity by macrophages. Cell. 1995; 80:353–361. [PubMed: 7530603]

63. Plummer T. Flaked stones and old bones: biological and cultural evolution at the dawn of technology. Am J Phys Anthropol. 2004; (Suppl 39):118–164. [PubMed: 15605391]
64. Raichlen DA, Alexander GE. Exercise, APOE genotype, and the evolution of the human lifespan. Trends Neurosci. 2014; 37:247–255. [PubMed: 24690272]
65. Schwarz F, Springer SA, Altheide TK, Varki NM, Gagneux P, Varki A. Human-specific derived alleles of CD33 and other genes protect against postreproductive cognitive decline. Proc Natl Acad Sci U S A. 2016; 113:74–79. [PubMed: 26621708]
66. Deutschman CS, Tracey KJ. Sepsis: current dogma and new perspectives. Immunity. 2014; 40:463–475. [PubMed: 24745331]
67. Hedlund M, Padler-Karavani V, Varki NM, Varki A. Evidence for a human-specific mechanism for diet and antibody-mediated inflammation in carcinoma progression. Proc Natl Acad Sci U S A. 2008; 105:18936–18941. [PubMed: 19017806]
68. Ruffell D, Mourkioti F, Gambardella A, Kirstetter P, Lopez RG, Rosenthal N, Nerlov C. A CREB-C/EBPbeta cascade induces M2 macrophage-specific gene expression and promotes muscle injury repair. Proc Natl Acad Sci U S A. 2009; 106:17475–17480. [PubMed: 19805133]
69. Lee B, Qiao L, Lu M, Yoo HS, Cheung W, Mak R, Schaack J, Feng GS, Chi NW, Olefsky JM, Shao J. C/EBPα regulates macrophage activation and systemic metabolism. Am J Physiol Endocrinol Metab. 2014; 306:E1144–54. [PubMed: 24691027]
70. Uematsu S, Kaisho T, Tanaka T, Matsumoto M, Yamakami M, Omori H, Yamamoto M, Yoshimori T, Akira S. The C/EBP beta isoform 34-kDa LAP is responsible for NF-IL-6-mediated gene induction in activated macrophages, but is not essential for intracellular bacteria killing. J Immunol. 2007; 179:5378–5386. [PubMed: 17911624]
71. Pizarro-Cerdá J, Desjardins M, Moreno E, Akira S, Gorvel JP. Modulation of endocytosis in nuclear factor IL-6(−/−) macrophages is responsible for a high susceptibility to intracellular bacterial infection. J Immunol. 1999; 162:3519–3526. [PubMed: 10092809]
72. Davies LR, Pearce OM, Tessier MB, Assar S, Smutova V, Pajunen M, Sumida M, Sato C, Kitajima K, Finne J, Gagneux P, Pshezhetsky A, Woods R, Varki A. Metabolism of Vertebrate Amino Sugars with N-Glycolyl Groups: resistance of α2-8-linked N-glycolylneuraminic acid to enzymatic cleavage. J Biol Chem. 2012; 287:28917–28931. [PubMed: 22692207]
73. van der Poll T, Levi M, van Deventer SJ, ten Cate H, Haagmans BL, Biemond BJ, Buller HR, Hack CE, ten Cate JW. Differential effects of anti-tumor necrosis factor monoclonal antibodies on systemic inflammatory responses in experimental endotoxemia in chimpanzees. Blood. 1994; 83:446–451. [PubMed: 8286742]
74. van Deventer SJ, Büller HR, ten Cate JW, Aarden LA, Hack CE, Sturk A. Experimental endotoxemia in humans: analysis of cytokine release and coagulation, fibrinolytic, and complement pathways. Blood. 1990; 76:2520–2526. [PubMed: 2124934]
75. Redl H, Bahrami S, Schlag G, Traber DL. Clinical detection of LPS and animal models of endotoxemia. Immunobiology. 1993; 187:330–345. [PubMed: 8330902]
76. Barreiro LB, Marioni JC, Blekhman R, Stephens M, Gilad Y. Functional comparison of innate immune signaling pathways in primates. PLoS Genet. 2010; 6:e1001249. [PubMed: 21187902]
77. Sibley CG, Ahlquist JE. The phylogeny of the hominoid primates, as indicated by DNA-DNA hybridization. J Mol Evol. 1984; 20:2–15. [PubMed: 6429338]
78. Patterson N, Richter DJ, Gnerre S, Lander ES, Reich D. Genetic evidence for complex speciation of humans and chimpanzees. Nature. 2006; 441:1103–1108. [PubMed: 16710306]

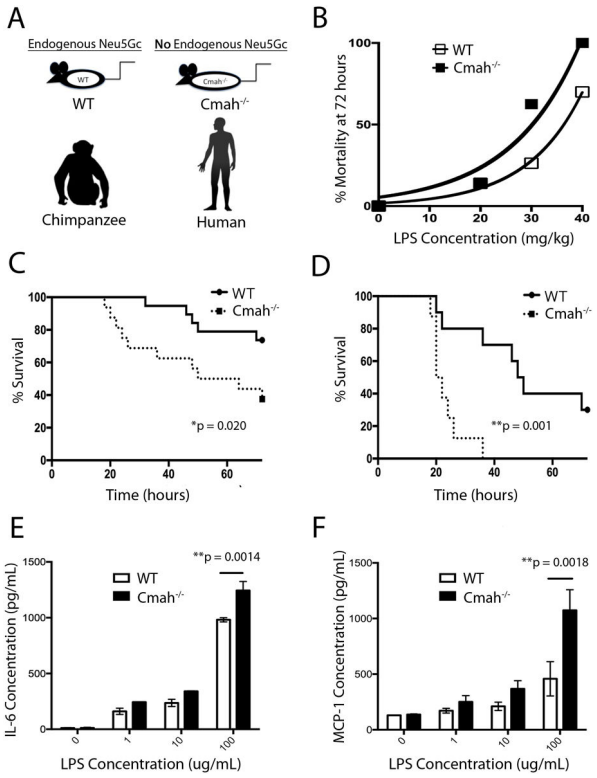

Figure 1. Comparison of the Inflammatory Response and Endotoxin Binding in WT and Cmah$^{-/-}$ mice

(A) Humans and *Cmah*$^{-/-}$ mice lack endogenous Neu5Gc, whereas WT mice and chimpanzees have high Neu5Gc expression. (B) Wild type and *Cmah*$^{-/-}$mice were subjected to lethal LPS challenge at different doses (20 mg/kg n=7, 30 mg/kg n=16, 40 mg/kg n=8) and % mortality at 72 hours was reported for each LPS concentration. (C) Wild type (n=19) and *Cmah*$^{-/-}$ mice (n=16) were subjected to lethal LPS challenge (30 mg/kg) (D) Wild type (n=8) and *Cmah*$^{-/-}$ mice (n=10) were subjected to lethal LPS challenge (40 mg/kg) and survival was monitored for 72 hours. (E) Bone marrow-derived macrophages (n=3) and (F) Peritoneal macrophages (n=4) from WT and *Cmah*$^{-/-}$ mice were stimulated for 24 hours with LPS and the secreted cytokines in the supernatant were quantified by cytokine bead assay (BD).

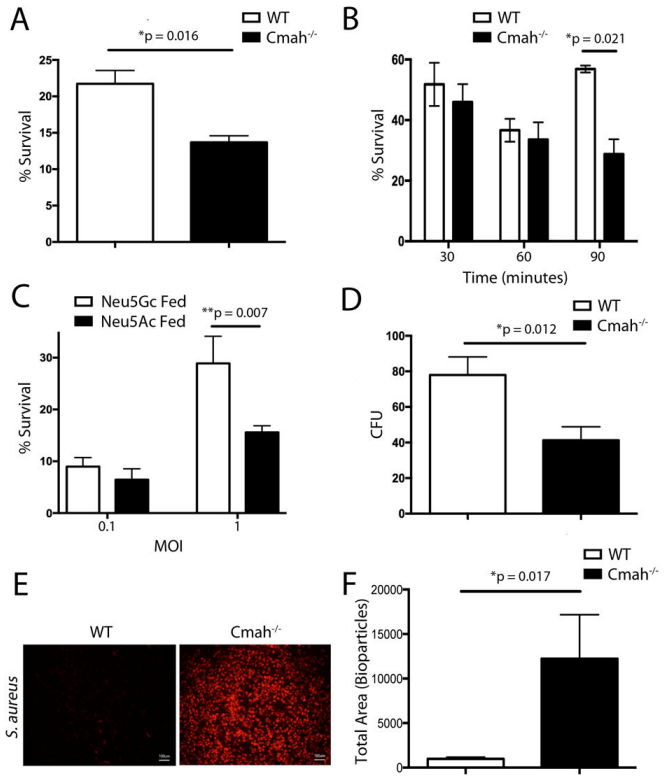

Figure 2. Comparison of Bacterial Killing and Phagocytosis in WT and Cmah$^{-/-}$ *ex vivo* and *in vivo*

(A) Peritoneal macrophages from WT and *Cmah*$^{-/-}$ mice were stimulated with *E. coli* K12 for 1 hour at an MOI of 1. (B) Whole blood from WT and *Cmah*$^{-/-}$ mice (n=3) was stimulated with ~4 × 10^5 CFU of *E. coli* K12 and aliquots were plated at 30 min, 60 min, and 90 min. (C) Peritoneal macrophages (n=4) from *Cmah*$^{-/-}$ mice were fed Neu5Ac or Neu5Gc for 4 days, followed by stimulation with *E. coli* K12 for 1 hour at MOI's of 0.1 and 1. (D) The lungs of WT (n = 9) and *Cmah*$^{-/-}$(n=8) mice were infected with 5 × 10^6 CFU of *E. coli* K12 and bacterial survival was assessed by plating an aliquot of the total lung homogenate 24 hours after infection. (E) Peritoneal macrophages from WT and *Cmah*$^{-/-}$ mice were stimulated with pHrodo Red *S. aureus* bioparticles for 2 hours. (F) Bioparticle fluorescence from WT and *Cmah*$^{-/-}$ mice was quantified by ImageJ (n=3).

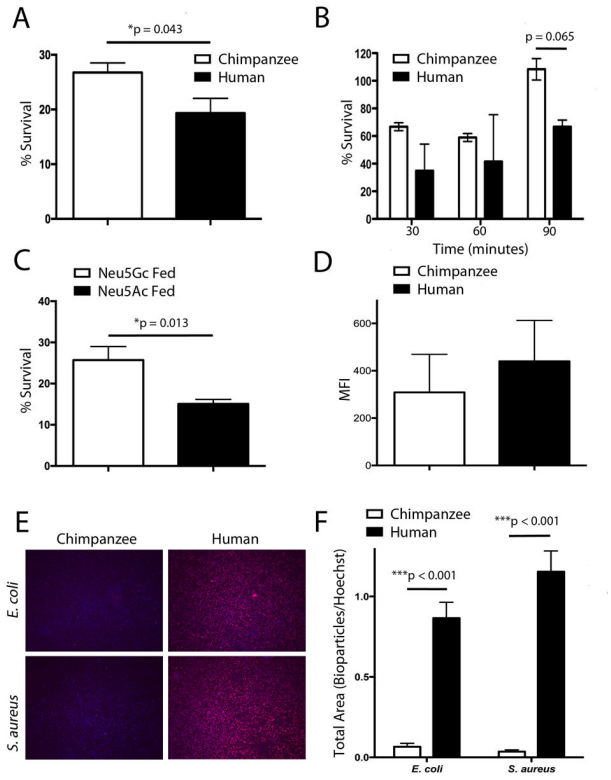

Figure 3. A. Comparison of Bacterial Killing and Phagocytosis in Humans and Chimpanzees

(A) Monocyte derived macrophages from humans and chimpanzees (n=6) were stimulated with *E. coli* K12 for 1 hour at an MOI of 1. (B) Whole blood from humans and chimpanzees (n=2) was stimulated with ~4 × 10^5 CFU of *E. coli* K12 and aliquots were plated at 30 min, 60 min, and 90 min. (C) Monocyte derived macrophages from humans (n=7) were fed 2 mM Neu5Ac or Neu5Gc for 4 days, followed by stimulation with *E. coli* K12 for 1 hour at an MOI of 1. (D) Monocyte derived macrophages from 5 humans and 4 chimpanzees were stimulated with 1 ng/mL LPS for 4 hours in the presence of Brefeldin A and intracellular TNFα expression was quantified by flow cytometry. (E) Monocyte derived macrophages from humans and chimpanzees were stimulated with pHrodo Red *E. Coli* or *S. aureus* bioparticles in pooled heat denatured autologous serum for 1 hour. (F) Bioparticle fluorescence from 5 humans and 4 chimpanzees was quantified by ImageJ.

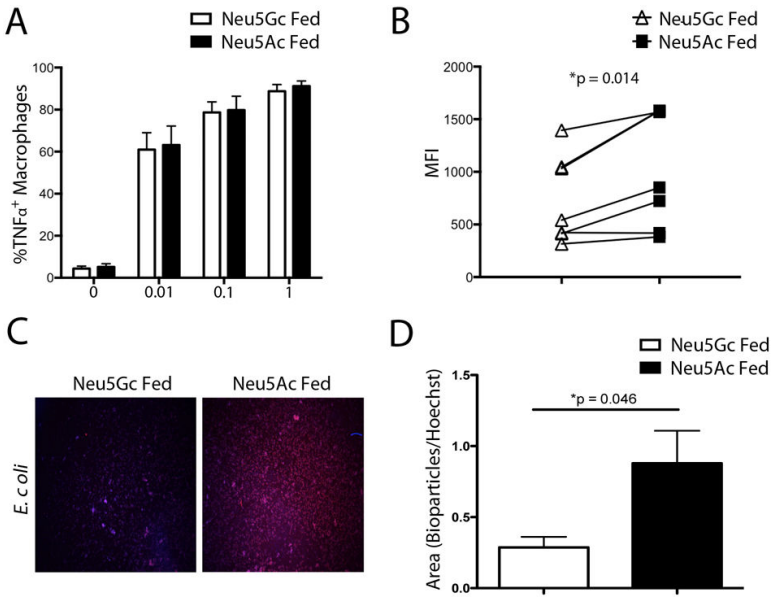

Figure 4. Comparison of TNFα production and Phagocytosis in Neu5Gc and Neu5Ac Fed Human Macrophages

(A) Monocyte derived macrophages from humans (n=7) were fed 2 mM Neu5Ac or Neu5Gc for 4 days, followed by stimulation with 0-1 ng/mL LPS in the presence of Brefeldin A for 4 hours and intracellular TNFα expression was quantified by flow cytometry. (B) At one concentration (1 ng/mL), the effect of Neu5Gc feeding was significant. (C) Monocyte derived macrophages were incubated with pHrodo Red *S. aureus* bioparticles in serum free conditions for 2 hours. (D) Bioparticle fluorescence from 4 individuals fed either Neu5Ac or Neu5Gc was quantified by ImageJ.

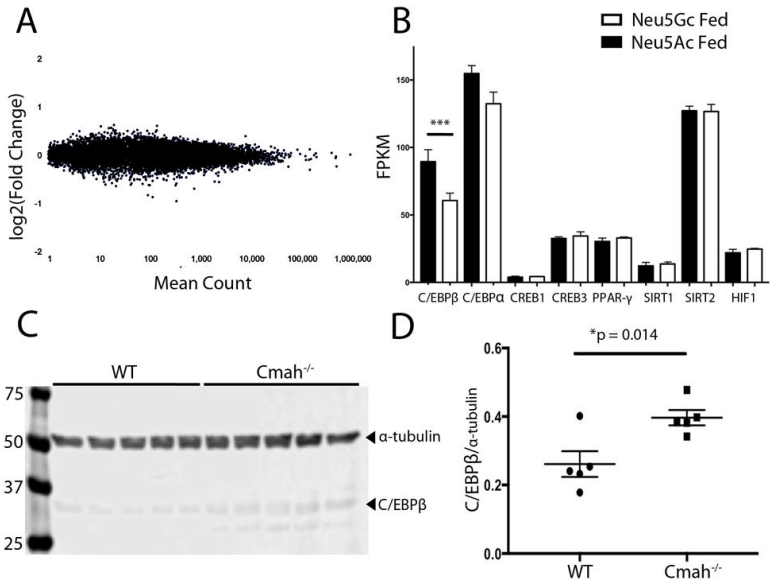

Figure 5. C/EBPβ Expression is Suppressed By The Presence of Neu5Gc

(A) MA plot of total RNA-seq results, comparing peritoneal macrophages isolated from Cmah$^{-/-}$ mice (n=3) fed either 2 mM Neu5Ac or 2 mM Neu5Gc for 3 days. (B) C/EBPβ expression was suppressed in macrophages that had been fed Neu5Gc (***q value = 0.000495 by DESeq analysis**)**. (C) Peritoneal macrophages from WT and Cmah$^{-/-}$ mice (n=5) were immunoblotted against α-tubulin and LAP, a 34 kDa isoform of C/EBPβ (background was subtracted in ImageJ with rolling ball radius of 100 pixels). (D) ImageJ quantification and analysis of WT vs. Cmah$^{-/-}$ LAP expression levels normalized to α-tubulin levels.